Annu. Rev. Mater. Res. 2003. 33:183–213
doi: 10.1146/annurev.matsci.33.022802.094122

First published online as a Review in Advance on February 26, 2003

RECENT ADVANCES IN MATERIALS FOR FUEL CELLS

N.P. Brandon,[1] S. Skinner,[2] and B.C.H. Steele[2]
[1]Department of Chemical Engineering, [2]Department of Materials, Imperial College, London, United Kingdom; email: n.brandon@ic.ac.uk; s.skinner@ic.ac.uk; b.steele@ic.ac.uk

Key Words materials technology, fuel cell stacks, reformers, SOFC, PEMFC

■ **Abstract** After a brief survey of fuel cell types, attention is focused on material requirements for SOFC and PEMFC stacks, with an introductory section on materials technology for reformers. Materials cost and processing, together with durability issues, are emphasized as these now dominate materials selection processes for prototype stack units. In addition to optimizing the cell components, increasing attention is being given to the composition and processing of the bipolar plate component as the weight and volume of the relevant material has a major influence on the overall power density and cost of the fuel cell stack. It is concluded that the introduction of alternative materials/processes that would enable PEMFC stacks to operate at 150–200°C, and IT-SOFC stacks to operate at 500–700°C, would have a major impact on the successful commercialization of fuel cell technology.

INTRODUCTION

General Comments

The behavior of many of the individual components incorporated into fuel cell stacks has been surveyed elsewhere in this volume, thus the main aim of this contribution is to examine additional constraints in materials selection introduced when a component is incorporated into a mass-produced fuel cell system. Manufacturing and operating costs, including reliability and durability, become paramount, and at present these factors usually restrict the commercial viability of fuel cell technology.

Information on fuel cell types and technology is provided by numerous books published in the last decade (e.g., 1–4). Useful historical surveys have been provided by Kordesch (5) and Appleby (6). Summaries of the current technological and commercial status of fuel cells are provided in the *Fuel Cell Handbook* issued by the U.S. Department of Energy (7), Proceedings of the Grove Fuel Cell Symposium (8), and Fuel Cells Bulletin (8a). Much useful information can also be downloaded from a variety of web sites (e.g., http://www.fuelcelltoday.com and links therein).

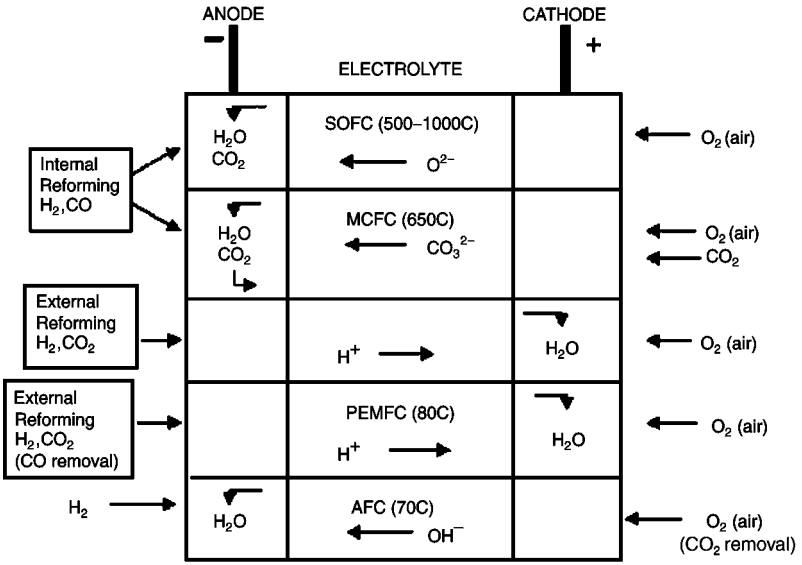

Figure 1 Summary of fuel cell types with typical reactants.

Discussions about the commercialization of fuel cell technology usually incorporate the five fuel cell types summarized in Figure 1 on the basis of the incorporated electrolyte. Examination of Figure 1 reveals that the lower-temperature systems—alkaline fuel cell (AFC), polymeric electrolyte membrane fuel cell (PEMFC), and phosphoric acid fuel cell (PAFC)—essentially operate on H_2 fuel, whereas the higher-temperature systems—molten carbonate fuel cell (MCFC) and solid oxide fuel cell (SOFC)—can also electrochemically oxidize CO, which is advantageous when a hydrocarbon fuel is supplied to the fuel cell. It should also be noted that the reaction products H_2O (and CO_2) are produced at the anode by AFC, MCFC, and SOFC cells but at the cathode by PEMFC and PAFC cells. This difference has a significant impact on the design strategies adopted for the various fuel cell systems. Moreover the choice of fuel is a further complication in the factors influencing the commercialization of fuel cells. This is illustrated in Figure 2. Whereas the low-temperature fuel cell types (PEMFC, PAFC) perform well with H_2 fuel inputs, the need to generate H_2 from a hydrocarbon feedstock such as natural gas introduces major equipment complexities, associated efficiency losses, and significant cost penalties. It is noted in passing that the AFC system cannot be operated on reformate gas mixtures owing to the presence of CO_2, which degrades the KOH electrolyte.

Materials selection for a commercial product involves an iterative design process that eventually becomes specific to the particular product and application. However, it is possible to make a few general statements about the selection of

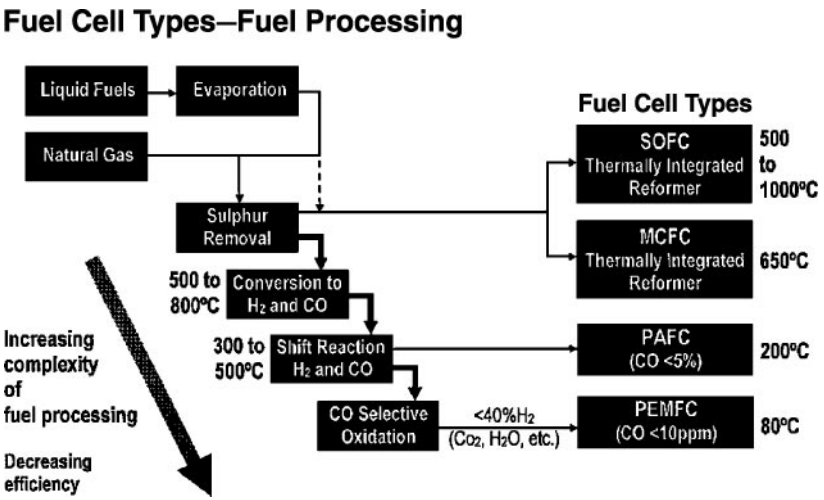

Figure 2 Fuel cell types and influence of fuel processing.

materials for fuel cell stacks. In addition to the technical requirements, economic considerations introduce major constraints because for many applications it is the capital cost ($/kW) and operating costs ($/kWh) that will determine whether fuel cell technology will succeed in displacing current technology.

Most observers (9) believe that for initial market entry the target cost/kW must be reduced to around $1000/kW, falling to below $500/$kW_e$ with volume production (10, 11). The capital cost of the stack will reflect the initial cost of the raw materials and their processing into a manufactured component ($/kg), multiplied by the amount of relevant material incorporated into the stack. The area-specific resistance (ASR Ωcm^2) of the individual cells is an important parameter because it influences the amount of material required (see Box A). It should be noted that fuel cells can be designed to be operated for maximum efficiency, maximum power, or some intermediate operating point that will optimize the cost/kWh. Although detailed stack models have been formulated to predict stack response to changes in operating conditions, a more useful simplified approach is to define relationships between fuel flow (an important operating cost), ASR, and operating voltage. These relationships can then be combined to create a closed form parametric model suitable for application in the construction of performance maps and operating point optimization and analysis. An example of this approach has been provided by Hartvigsen et al. (12), assuming isothermal conditions for a natural gas–fueled SOFC operating at 800°C. For H_2O/CH_4 ratios of 2, and an ASR value of 0.5 Ω cm^2, the stack power drops approximately by a half, from the point of maximum power to the point of maximum efficiency. However, the actual values depend crucially on the selected ASR value.

Box A

The overall cell efficiency η is given by the equation

$$\eta = \eta_g \eta_v \alpha,$$

where η_g is the Gibbs efficiency, η_v is the voltage efficiency, and α is the fraction of fuel used.

$$\eta_g = \Delta G/\Delta H = nFE_0/\Delta H, \qquad \eta_v = E/E_0 = (E_0 - IR_c)/E_0,$$

where E_0 is the open circuit voltage, and ΔH is the heat of the overall cell reaction. Thus

$$\eta = nF(E_0 - IR_c)\alpha/\Delta H,$$

where R_c is the area-specific resistivity (ASR) of the cell components (electrolyte, anode, and cathode)

$$\text{Power} = IE = I(E_0 - IR_c).$$

The cell ASR is thus an important parameter having a major influence on the cell efficiency and specific power (W/cm^2) output. These terms then influence the operating and capital cost of the fuel cell system.

The electrochemical oxidation of a fuel can, in theory, be accomplished at very high efficiencies (e.g., 83% for the H_2/O_2 reaction at 25°C) compared with heat engines utilizing the combustion of a fuel. However, in practice, fuel cells also experience irreversible losses due to resistive and polarization losses (see Figure 3), and efficiencies of fuel cell stacks rarely exceed 50–60%. The irreversible losses appear as heat, and, for example, a 1 kW fuel cell operating at 50% efficiency also has to dissipate 1 kW of heat. Although high power densities (1 W cm^{-2}) have often been demonstrated in the laboratory, thermal management considerations for the fuel cell system usually restrict the maximum power density in the stack to around 0.5 W cm^{-2} at 80–90% fuel utilization. Thermal management of fuel cell stacks is thus an important design consideration requiring careful selection of cooling fluid and associated materials. For a fuel cell operating around 0.7 V, a power output of 0.5 W cm^{-2} requires a current density of at least 0.7 A cm^{-2}. If the OCV is 1 V, then the allowed voltage loss (0.3 V) can be achieved only if the ASR value does not exceed ~0.45 Ω cm^2 (0.3/0.7). For a single cell assembly this implies target ASR values of 0.15 Ω cm^2 for the individual cathode, anode, and electrolyte components (this value is used in subsequent sections). To generate technologically useful voltage outputs from the stack, many individual cells are usually connected together in series, using impermeable electronic-conducting interconnects or bipolar plates, which often also distribute the reactant gases to the respective porous electrodes.

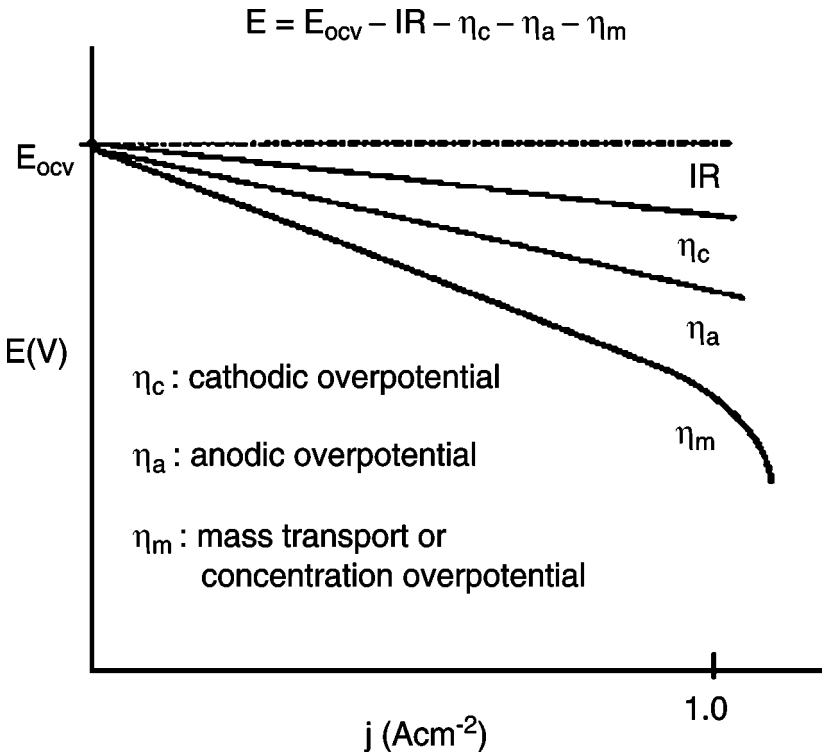

Figure 3 Current-voltage characteristics of fuel cells.

These components can also introduce resistive losses, often via contact resistivities, and much effort is usually required to minimize these resistivities (as discussed below).

As discussed elsewhere by one of the authors (13), innovations in materials technology are mainly associated with the PEMFC and SOFC systems, and accordingly in subsequent sections attention is focused on these fuel cell types, which at present still appear to have opportunities to satisfy their commercial opportunities. It is of note that the materials presently being used in the PEMFC and tubular SOFC prototype demonstration units are essentially the same as those selected at least 25 years ago (3, 4). Although innovative fabrication and processing routes have improved their attributes (e.g., lower cost, lower Pt loadings), it is only in the past five years that system engineering and commercialization issues have highlighted the inadequacies of some of the materials originally selected. As indicated in the following sections, it is these issues that are now driving the development of alternative materials, particularly for the PEMFC and intermediate temperature (IT) SOFC stacks.

Fuel Choice and Fuel Storage

It is important to recognize that the type of fuel and its storage have important ramifications for both fuel cell technology and associated materials development. Although the lower-temperature fuel cell systems exhibit excellent performance with pure H_2, this fuel is relatively expensive to produce, and its storage incurs large gravimetric and volumetric energy density penalties (14). Clearly, if a novel hydrogen storage material can be developed with a reversible capacity approaching 10% by weight of hydrogen, then there would be a paradigm shift in attitudes to hydrogen fuel and the hydrogen economy. However, until this occurs, fuel cells for transport will probably be provided with liquid fuels such as gasoline or methanol, whereas stationary fuel cells for combined heat and power (CHP) will be supplied with natural gas and liquid petroleum gas (LPG) products, although other fuels such as dimethyl ether (15) are also being examined. This scenario introduces problems for the low-temperature fuel cells because an external fuel processor must be incorporated into the system to produce the hydrogen (see Figure 2). This not only increases the cost and complexity of the unit but also reduces the overall efficiency. External fuel processors (reformers) are also the subject of intensive development around the world, and a variety of innovative compact reformers using diffusion-bonded printed circuit components or micro-channel designs (16) also illustrate the impact of materials technology on this aspect of fuel cell systems. Further comments on materials aspects of reformers are provided in a subsequent section.

Other Considerations

Additional constraints influencing material selection arise from reliability/durability issues. For transport applications, target performance degradation values (e.g., 0.1% over 1000 h) are required for projected operational life-times of 5000 h. However, for stationary applications (e.g., distributed CHP), a similar degradation rate must extend over a period of at least 40,000 h (5 years). These different life-time targets introduce problems for PEMFC prototype CHP systems because the stack components were originally developed for transport applications.

Durability issues can be a particular problem for high temperature SOFC stacks owing to interfacial reactions between adjoining components and the proliferation of gaseous species such as $CrO_2(OH)_2$, which can transport cations into critical electro-active components such as cathodes. Performance degradation due to impurities such as SiO_2 has often been described (e.g., 17), and the role of impurities on electrode kinetics was emphasized in a recent report by Morgensen et al. (18). These authors suggest that most of the conflicting reports about SOFC electrodes can be attributed to variable amounts of impurities introduced from the raw materials and fabrication procedures in different laboratories. Also of great relevance are the investigations of de Ridder et al. (19) into the rate-limiting step for SOFC cathodic kinetics. They propose that the outermost surface (atomic layer) of YSZ plays a dominant role in the overall cell performance, and these authors

highlight the segregation of Y_2O_3 to the surface and the associated decrease in oxygen surface exchange kinetics.

A fuel cell system also incorporates relevant balance-of-plant items such as pumps, valves, heat exchangers, piping, electronic controls, DC/AC inverters, etc. Materials aspects of these components, which can be responsible for at least half the cost of a fuel cell system, are not considered further here, but the relevant chapter in the U.S. DOE Fuel Cell Handbook (7) provides a useful introduction to this topic. It should be noted that for the PAFC system, many of which have now been operated for periods approaching 30,000 h, the main source of system breakdown has been balance-of-plant items. External fuel processors (reformers) are also the subject of intensive development around the world and are the subject of an introductory survey (see below).

MATERIALS FOR SOFC STACKS

General Comments

SOFC technology has been under development for over forty years, and it is not surprising that all the prototype demonstration systems incorporate the same materials for the PEN (positive cathode, electrolyte, and negative anode) components, namely La(Sr)MnO_3 (LSM), yttria stabilized zirconia (YSZ), and Ni/YSZ composite anodes. An excellent review in 1997 by Kawada & Yokokawa (20) discusses the scientific basis for the PEN compositions, often selected as a result of empirical development programs, and later surveys (21, 22) incorporate more recent advances. Although similar compositions are usually selected, the specific manufacturing process chosen reflects the particular stack configuration (e.g., tubular, planar, etc.). The temperature of operation and stack configuration also determine the material selected for bipolar plate/interconnect. The fabrication routes used by companies worldwide for the prototype demonstration units have been usefully surveyed by Tietz et al. (23), and the reader is recommended to consult the compilations incorporated in this reference.

TUBULAR CONFIGURATIONS For the tubular concept, the cathode (or a porous inert composition) is often used as the support substrate, and at present relatively expensive processes (electrochemical vapor deposition, plasma spraying) are used to deposit the YSZ electrolyte film (typically 40 μm thick). However, the cost targets are difficult to achieve with these techniques, even at MW plant size, and a variety of slurry processes are under active development. A brief survey of alternative fabrication techniques has been compiled by Will et al. (24), but it should be noted that many of these are more appropriate for academic laboratories than for cost-effective, commercial mass production. The configuration adopted by Rolls-Royce (25) attempts to overcome some of these cost penalties by using a segmented series arrangement of individual cells deposited by a relatively cheap screen-printing process. Although similar in concept to one of the original tubular

Westinghouse configurations (26), the Rolls-Royce porous spinel substrate has a rectangular cross-section that makes possible the use of conventional ceramic processing methods such as screen-printing. It should be noted that the fabrication of a PEN assembly usually requires several high-temperature processing steps, and it is important that these are arranged in an appropriate sequence to avoid interfacial degradation such as the formation of $La_2Zr_2O_7$, $SrZrO_3$, at the cathode/electrolyte interface. An example is provided by the Siemens-Westinghouse manufacturing route in which the interconnect material, $La(Ca)CrO_3$, which requires a relatively high temperature to densify, is deposited before the electrolyte film. Most large-scale prototype tubular systems use the ceramic-doped $LaCrO_3$ interconnect, which fulfills many of the relevant requirements including stability in oxidizing and reducing environments. However, the thermal conductivity is low (<5 W m^{-1} K^{-1}), and doped $LaCrO_3$ exhibits different thermal expansion coefficients (TEC) in oxidizing and reducing environments because of changes in the oxygen stoichiometry. It follows that high heating rates should be avoided to ensure that any thermal stresses developed can be tolerated. Fortunately, most applications of the tubular configuration will involve relatively large (>1 MW) stationary plants, in which the SOFC stack is coupled to a turbine to guarantee that electricity is generated at efficiencies approaching 70%. Such plants do not require high heating rates, and procedures can be adopted to ensure that unusual operating conditions (e.g., loss of load, fuel supply, etc.) do not impose severe thermal stresses on the ceramic stack. From an engineering aspect, the Siemens-Westinghouse stack technology has many attractive features, including lack of high temperature seals with cell degradation rates as low as 0.25%/1000 h of operation being reported, and most development is now focused on cost reduction of the processing routes.

In an effort to avoid some of the processing and operational restrictions, such as low tolerance to thermal stresses associated with the Siemens-Westinghouse technology, efforts have continued to develop tubular systems based on single tubes using external current collectors and interconnects. Such developments were stimulated in the early 1970s by the fabrication of thermal shock resistant partially stabilized zirconia tubes for oxygen sensors designed to be rapidly immersed into molten copper at 1100°C, and Russian developers (27) constructed 1-kW units for tele-metering operation at remote locations such as oil/gas pipelines. In the mid 1990s, Kendall & Sales (28) introduced small-diameter, thermal, shock-resistant YSZ tubes, and small stacks continue to be developed by Acumentrics (29) and Adelan. However, a significant problem with this configuration continues to be the lack of a cheap, durable, cathode current collector material. At present Ag appears to be the favored choice, but this material was rejected (30) in the 1960s because of cost and high Ag vapor pressure at the elevated operating temperatures.

PLANAR SYSTEMS Initially planar SOFC configurations were based around self-supported ($\sim$150 μm) YSZ electrolytes, which required operating temperatures in excess of 950°C to avoid excessive resistive losses associated with the electrolyte component (see Figure 4). Operation at 950°C introduced significant problems,

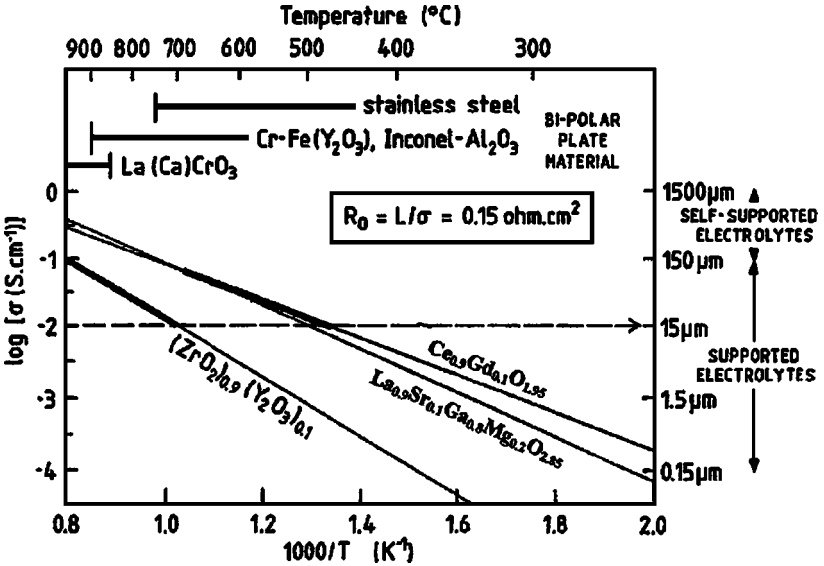

Figure 4 Specific conductivity versus reciprocal temperature for selected solid oxide electrolytes.

including stability of the electrolyte/cathode interface and selection of the bipolar plate material and the optimal material composition for the seals that are necessary in planar SOFC stacks. Fortunately by 1990, came the realization that for smaller SOFC stacks not designed to be integrated with gas turbines the operating temperature should be lowered as far as possible without compromising the electrode kinetics and internal resistance of the cell. Examples of the most appropriate solid electrolyte composition for operation at intermediate temperatures (500–750°C) can be identified from Figure 4. Assuming again that the electrolyte component should not contribute more than 0.15 Ω cm^2 to the total cell ASR, then for a thick film thickness (L) of 15 μm the associated specific ionic conductivity (σ) value of the electrolyte should exceed 10^{-2} S cm^{-1} ($\sigma = L/\text{ASR} = 0.0015/0.15$). Examination of Figure 4 indicates that the ionic conductivity of YSZ attains this target value around 700°C, and for $Ce_{0.9}Gd_{0.1}O_{1.95}$ (CGO) the relevant temperature is 500°C. The use of thinner electrolyte films would allow the operating temperature to be lowered. However, at present it appears that the minimum thickness for dense impermeable films that can be reliably mass-produced using relatively cheap ceramic fabrication routes is around 10–15 μm. The use of a thick film electrolyte requires this component to be supported on an appropriate substrate. As the substrate is the principal structural component in these cells, it is necessary to optimize the conflicting requirements of mechanical strength and gaseous permeability.

Most development work on planar IT-SOFC systems has involved YSZ electrolyte thick films, and so far most groups have used anode (Ni-YSZ) substrates

(23), which allows the electrolyte powder to be densified around 1400°C. One of the problems associated with using porous composite Ni-YSZ substrates is its relatively poor thermal expansion compatibility with the YSZ thick film. Accordingly, several groups are examining porous substrates based on Ni-Al_2O_3 or Ni-TiO_2 compositions with thin Ni-YSZ-CeO_2ss interfacial anodic regions. Although replacement of the YSZ can provide better thermal expansion compatibility, problems still remain over the volume changes associated with the reduction/oxidation of the Ni component. As the porous substrate/electrolyte films are usually co-fired in air around 1400°C, nickel is present as NiO, which has to be carefully reduced by the fuel during the initial heating cycle of the assembled stack. It should also be noted that operating procedures have to be specified to prevent the nickel re-oxidizing when SOFC stacks are cooled down without fuel flowing through the anode compartment (c.f., use of forming gas, N_2/H_2, to protect the Ni-YSZ anode in the Siemens-Westinghouse tubular configuration).

Most stack IT-SOFC developers are using metallic bipolar plates as the interconnect component. Initially, a Cr5%Fe (1%Y_2O_3) oxide dispersion–strengthened alloy was developed for 950°C operation, but now most prototype stacks incorporate a ferritic stainless steel (23) as the bipolar plate because of the low ($12.5 \times 10^{-6}\ K^{-1}$) TEC of these alloys. At present, the optimal composition of the alloy remains uncertain owing to conflicting requirements for the oxide coating formed on these alloys. An appropriate protective film has to be formed to withstand the oxidizing (cathode compartment) and the high steam content developed in the anode compartment. In addition, the oxide layer has to exhibit sufficient electronic conductivity at the operating temperature to ensure that contact area-specific resistivities (ASR) resistances are below 10 $m\Omega cm^2$. Some special alloys (e.g., Krupp JS-3 and Hitachi ZMG 232) containing small quantities of La and Mn (31, 32) have been developed, but at present the performance of these semi-commercial alloys do not appear to offer significant advantages over selected alloys (e.g., DIN 1.4905) already commercially available (33).

Another problem associated with the ferritic steels is the transport (34) of Cr gaseous species [e.g., CrO_3, $CrO_2(OH)_2$, $Cr(OH)_3$] into the porous cathode and anode components and subsequent formation of deleterious phases such as $MnCr_2O_4$ and $NiCr_2O_4$, which can severely degrade the electrode performance. At present most developers are reducing the Cr activity by coating the steel with films of doped $LaCrO_3$ using plasma-spraying techniques (35), but a reduction in operating temperature to below 700°C would probably be the optimal solution.

Providing that appropriate precautions are followed, many development laboratories have reported (36) good performance values for IT-SOFC stacks incorporating the following PEN components: anode-supported thick film YSZ electrolytes, LSM-YSZ cathodes, and stainless steel bipolar plates. To minimize sealing requirements, many IT-SOFC stack developers have adopted a circular design in which the fuel and air are introduced via an appropriate manifold at the center of the PEN structure (e.g., 37). These design features minimize sealing problems and allow limited thermal cycling. However, the heating/cooling rates at present cannot

exceed about 500°C/h owing to stresses associated with thermal expansion mismatch and the brittle glass/ceramic seals. Although this restriction may not be too severe for larger CHP systems (>100 kW), it is not satisfactory for smaller systems (1–10 kW) designed for micro-CHP and auxiliary power unit applications. Further research and development is still required to produce more rugged IT-SOFC stacks. In this context, attention is drawn to the thick film planar SOFC units deposited on a porous metallic substrate by multistep vacuum plasma spraying (38) and by conventional ceramic-processing routes (39). Commercial units can be expected in the next five years once reliability and cost requirements (<$1000/kW) have been effectively demonstrated.

Although YSZ is still the favored electrolyte material for SOFC stacks, selection of this material is not without problems, and alternative electrolyte materials are being considered. The use of ceria-based electrolytes such as $Ce_{0.9}Gd_{0.1}O_{1.95}$ (CGO) should in principle allow the cell-operating temperature to be lowered to around 500°C (see Figure 4). However, perceived problems associated with PEN structures incorporating ceria-based electrolytes have restricted investment in this technology. It is well known that at elevated temperatures Ce^{4+} ions can be reduced to Ce^{3+} under the fuel-rich conditions prevailing in the anode compartment. The associated electronic conductivity (and deleterious lattice expansion) produces an internal short circuit in the PEN structure that can significantly degrade the efficiency and performance of cells incorporating ceria-based electrolytes. However, as emphasized earlier (40) if the operating temperature is lowered to around 500°C, then the electronic conductivity contribution is small and can be neglected under typical cell-operating conditions. Operation at 500°C allows the use of compliant high-temperature gaskets in place of rigid, brittle glass/ceramic seals thus permitting greater design flexibility for the stack configuration. At Imperial College we also take advantage of the fact that the TEC of CGO and ferritic stainless steel are virtually identical (12.5×10^{-6} K^{-1}) and thus the thick film PEN structure can be supported on a porous stainless steel foil. Fabrication routes are also being developed (40a) to ensure that the processing procedures do not exceed the annealing temperature (1000°C) of the stainless steel. These metal-supported PEN structures are robust and should withstand the rapid temperature cycles expected during operation of small IT-SOFC stacks. Obviously, IT-SOFC stacks operating at 500°C offer some exciting possibilities, and it is important that 1-kW stacks be demonstrated as soon as possible.

Another serious difficulty that has restricted exploitation of the attractive properties of CGO at 500°C has been the need to develop alternative electrode compositions that function effectively at this temperature, and this topic is considered in the next section.

Another electrolyte, doped $LaGaO_3$ (LSGM), is also attracting much attention for IT-SOFC applications. Although its conductivity is slightly less (see Figure 4) than CGO at 500°C, its ionic domain is wider, and it could be more appropriate to use this electrolyte at temperatures around 600°C, where the reduction of Ce^{4+} in CGO is becoming significant. It has been difficult to fabricate pure single-phase

ceramic electrolytes, and second phases such as $SrLaGa_3O_7$ and $La_4Ga_2O_9$ are often detected in the grain boundaries. Whether these phases are responsible for the enhanced reactivity of doped $LaGaO_3$, or whether it is an intrinsic property of doped $LaGaO_3$, are questions that require answers as soon as possible. Moreover the preferred composition, $La_{0.9}S_{r0.1}Ga_{0.8}M_{g0.2}O_{2.85}$, does not appear to be stable at lower temperatures (41). Mention should also be made of the composite electrolytes reported by Meng et al. (42). These investigators have fabricated composite CGO/carbonate electrolytes with transport properties that are enhanced compared with those of the simple CGO materials. However, these electrolytes are probably better considered as molten carbonates immobilized in a CGO matrix. Although research continues into the synthesis of alternative oxygen ion-conducting electrolytes (see Goodenough this volume) (42a), it has proved difficult to prepare alternative materials with an appropriate combination of properties and cost attributes that can displace the traditional fluorite compositions involving ZrO_2 and CeO_2.

SOFC Electrodes

Of critical importance to the efficiency and operation of commercial SOFC devices are the electrodes. Each electrode, that is cathode and anode, has demanding materials selection criteria, and, indeed, when selecting an electrode material, consideration has to be given to the compatibility with the relevant electrolyte. The following sections provide a discussion of both the anode and cathode materials proposed for use in SOFC stacks.

ANODES The conditions under which a typical SOFC anode would operate are technically demanding, both in terms of the electrochemical requirements for the material and its stability within the reducing conditions present at the anode. To meet these requirements it was necessary to develop cermet anodes, typically with Ni and the appropriate electrolyte material, i.e., YSZ or CGO. Of significance to this development is the cermet microstructure, and hence the route used to produce such materials is important. Recent work (43) has suggested that a combustion synthesis route based on the well-known citrate-nitrate solution route could produce ultrafine Ni-YSZ cermets suitable for anode manufacture. Marisnek et al. considered the effects of synthesis conditions on the final cermet material microstructure and conductivity. Ringuede et al. (44) have also investigated the combustion synthesis route in preparing cermet anodes and assessed the anodes thus prepared through electrochemical impedance spectroscopy and examination of the microstructure. These authors report a polarization resistance of $\sim 1\ \Omega\ cm^2$ at $\sim 900^\circ C$ and good microstructural features consistent with anodes produced via conventional synthesis routes. Further alternative synthesis routes for the production of Ni-YSZ cermets have been reported with a spray pyrolysis technique (45), producing anodes with stable cell voltages of ~ 0.8 V in humidified H_2 over a long-term test period of 8000 h.

Typically, the anode material used in SOFC prototype demonstration units has been limited to the Ni-YSZ cermet in order to achieve the necessary electrical performance and stability in the fuel conditions present. As the fuel requirement increasingly focuses on hydrocarbon fuels with lower steam ratios, the specification for the anode alters. Increasingly, discussions regarding anode materials are highlighting the direct oxidation of hydrocarbon fuels at the anode, for which the traditional Ni-based cermets are unsuitable owing to carbon deposition. This topic is discussed by Mogensen (see Mogensen & Kammer this volume) (45a), but a recent publication (46) illustrates the type of approach being adopted by developers.

Cermet anodes based on CGO are also attractive candidates (47) for use in SOFCs based on a CGO electrolyte, and to this end Hibino et al. (48) have investigated some noble metal-doped Ni-CGO anodes. The addition of the noble metal acts as a catalyst for the reforming of the fuel, and an optimal noble metal-loading of 3 wt% Ru was determined. These authors have developed a Ni-ceria samaria anode ($Ce_{0.8}Sm_{0.2}O_{1.9}$) that, when doped with Pd as a catalyst, has very encouraging performance at the remarkably low temperature of 550°C with a power density of 640 mW cm^{-2}. Alternative optimization of ceria-based anodes has included the development of La_2O_3-doped CeO_2 (49). A composition of 40 mol% La_2O_3-doped CeO_2 with NiO appears to be competitive as an anode, and a further improvement in cell performance occurred when cells were produced with Ni-free interlayers. Maximum power density at 800°C was found to be 900 mW cm^{-2}, and an overall cell ASR of 0.34 Ω cm^2 was reported.

Several authors (e.g., 50–60) have reported studies of alternative ceramic-based anodes, and Liu et al. (54) in particular claim a fuel-flexible anode composed of a lanthanum chromite perovskite, CGO, and a small amount of Ni metal in what could be viewed as a composite anode. A variety of compositions were screened on a CGO electrolyte-based SOFC with H_2, CH_4, C_3H_8, and C_4H_{10} fuels, and stable performance was achieved with all fuels. Hui & Petric (52) also opted for the ceramic approach to anode development and have evaluated yttria-doped strontium titanate, both in terms of fuel cell performance and chemical compatibility with traditional electrolytes, but report poor power densities even at elevated temperatures of 900°C. However, Marina & Pederson (62) report useful power densities with a composite anode incorporating $(La,Sr)(Ti,Ce)O_3$. Continuing with the investigation of perovskite anodes, Kunifusa et al. (63) report that a $Nd(Cr_{1-x}Mg_x)O_3$ anode has excellent electrical conductivity, but there are no data for cell testing. It has also been suggested (64) that $La_{1-x}Sr_xCr_{1-y}Ru_yO_3$, where $0.2 \leq x \leq 0.4$, $0.05 \leq y \leq 0.2$, would be suitable for use as an anode under a methane fuel, particularly given the affinity of Ru for catalyzing the decomposition of methane.

CATHODES Significant advances have been made in recent years in the development of cathode materials (65), and it is now essential that efforts are directed toward the optimization of the cathode fabrication and structure. One of the more significant advances in cathode construction has been the introduction of functionally graded materials, as discussed by Hart et al. (66, 67). In this case, a

cathode composed of a four-layer structure of varying mixtures of YSZ or CGO, LSM, and $La_{1-x}Sr_xCoO_{3-y}$ (LSC) was deposited upon a YSZ tile. The outer layer in this structure is an LSC current collector produced through tape casting, whereas the preceding layers, $\sim$10 μm thick, are deposited by spraying. Both YSZ- and CGO-based functionally graded cathodes were investigated, and only at low temperatures were significant differences found, with the CGO system having an ASR of 6.83 Ω cm^2 at 750°C compared with the 11.36 Ω cm^2 for the YSZ-based system. Holtappels & Bagger (68) have advanced this concept using multi-layer graded cathodes with up to nine layers in the cathode structure.

A further development of the functionally graded cathode concept has been reported by Xia et al. for use in a novel honeycomb fuel cell (69). It is claimed that the honeycomb design overcomes the manifolding and sealing difficulties associated with planar designs and low-power densities achieved with tubular designs. Using the graded cathode, Xia et al. (69) have achieved a polarization resistance of 0.47 Ω cm^2 at 750°C for a LSM-based design graded with CGO. It was also reported that lowering of the sintering temperature for this cathode structure significantly improved the polarization resistance.

An alternative approach has been adopted by Yoon et al. (70) in the preparation of single cells based on the YSZ-LSM system. The authors have used a slurry coating technique to deposit a cathode layer of $\sim$60 μm thickness on a YSZ substrate. After the LSM film was dried and sintered, the cathode was dip coated with either YSZ or SDC and calcined at 600°C. This technique produced thin film coatings of the electrolyte material within the pores of the cathode. The authors report that by building up a coating by repeatedly dip-coating, a significant improvement in the power density was observed when compared with that of LSM cathodes prepared by conventional (e.g., screen-printing) techniques.

Much work continues on the optimization of La-based perovskites for cathodic applications (71, 72), and Simner et al. (73) have evaluated a series of ferrites for anode-supported designs with a view to operating a cell in the 650–800°C range. This work suggested that the LSF20 composition ($La_{0.8}Sr_{0.2}FeO_{3-\delta}$) is optimal and that further B site doping degrades the material performance; however, the power density achieved is low at the lower temperature regime. In the same vein, Dasgupta et al. (74, 75) investigated the neodymium analogues, $Nd_{1-x}Sr_xFe_{1-y}Co_yO_3$, of the LSCF series, which have been reported to exhibit good activity toward oxygen reduction (76). Dasgupta et al. focused primarily on the structural aspects of these compositions but reported attractive values for the conductivity and TEC. In the Co-doped materials, peak conductivity of 320 S cm^{-1} at 627°C was achieved for the $Nd_{0.7}Sr_{0.3}Fe_{0.2}Co_{0.8}O_3$ composition. The TEC of this series of materials was found to be similar to the LSC analogues, with values varying from 11 to 20 $\times$ 10^{-6} K^{-1}. As with the La-doped materials, the higher Co content materials suffer from high TEC values.

Further development of the perovskite-type oxides has identified the $Ba_{1-x}La_xCoO_3$ (77) composition as an attractive material for use on $La_{1-x}Sr_xGa_{1-y-z}Mg_yCo_zO_{3-\delta}$ electrolytes with an optimal performance of 550 mW cm^{-2} at 800°C. In

terms of power density, the barium cobaltites have proved to be slightly better as cathodes than the analogous $Sm_{1-x}Sr_xCoO_3$, particularly at intermediate temperatures where the overpotential of the $Ba_{1-x}La_xCoO_3$ is smaller than for the $Sm_{1-x}Sr_xCoO_3$. $Sr_{0.25}Bi_{0.5}FeO_{3-\delta}$ has also been proposed as a cathode composition (78), although the polarization resistance of this material at 800°C is relatively high at 2.16 Ω cm^2. Kharton et al. (79, 80) and Patrakeev et al. (81) report the preparation of (La,Sr)(Fe,Ga)$O_{3-\delta}$ and discuss the oxygen conductivity of a range of compositions. A peak total conductivity for the $La_{0.3}Sr_{0.7}Fe_{0.8}Ga_{0.2}O_{3-\delta}$ composition of $\sim$100 S cm^{-1} was found with peak oxide ion conductivity of 0.25 S cm^{-1} reported at 600°C. The higher gallium contents were found to lower the activation energy for conduction.

Perovskite-related materials, particularly of the K_2NiF_4 structure type, have also been investigated as possible cathode materials (82–88). In particular, the $La_{2-x}Sr_xNi_{1-y}M_yO_{4+\delta}$ compositions, where M = transition metal, have recently been investigated with work focusing on the oxide ion diffusion and oxygen permeation characteristics of these materials. Interest in these materials stems from the high interstitial oxygen content, which has been reported to lead to fast oxygen diffusion characteristics (86, 87). Testing of these materials, and in particular the Pr and Nd analogues as cathodes on a YSZ electrolyte, has produced encouraging results with polarization resistance values two orders of magnitude better than the perovskite $La_{1-x}Sr_xFe_{1-y}Ni_yO_{3-\delta}$ at 650°C (84).

Additional work has also been concerned with the production and optimization of composite cathodes (90–94). A variety of composite cathodes have been produced that mainly consist of a perovskite oxide and noble metal or an electrolyte/cathode. Of these, Barbucci et al. (91) investigated both types looking at Pt/YSZ and LSM/YSZ by impedance spectroscopy and found that, in terms of conductivity, the LSM/YSZ composite is approximately one order of magnitude better than the noble metal-based material. Wang et al. (92) investigated a LSCF/CGO/Ag composite on ceria samaria oxide and concluded through impedance measurements that at temperatures below 700°C and on a ceria-based electrolyte this composition is an excellent candidate for a workable cathode. However, little structural work has been performed and the cathode composition has not been optimized. Fukui et al. (94) investigated the incorporation of nanoparticles in a LSM/YSZ composite electrode. This electrode had a good open porous structure, exhibiting excellent electrochemical activity, and the authors reported a cathode polarization of 120 mV at 500 mA cm^{-2}. The LSM/YSZ couple has also been used as the basis of a multilayer cathode structure proposed by Holtappels & Bagger (68). Further investigations of the LSCF/CGO composite has been carried out by Perry-Murray et al. (93), again using impedance spectroscopy and building on earlier work by other groups (95). In broad agreement with the earlier work, it was found that 50 vol% CGO added to LSCF improved the interfacial resistance substantially and that values of $R_i = 0.01$ Ω cm^2 at 750°C were achieved on a YSZ electrolyte. The authors highlight the possibility that this combination of components looks attractive for low-temperature SOFC operation (<600°C).

Although cathodic kinetics are often interpreted in terms of the classical Butler-Volmer model, Adler et al. (96) proposed an alternative approach in which heterogeneous reactions within a porous, mixed-conducting electro-catalyst can be responsible for the major contribution to the polarization voltage. This model has the advantage that ASR values for cathodes can be predicted from materials parameters (microstructural features, oxygen self-diffusion, and surface exchange coefficients). Where relevant data are available, good agreement has been reported (97) between calculated and measured ASR values. Oxygen diffusion and surface exchange coefficients can change the magnitude of the ASR value by orders of magnitude, and a selection of appropriate oxygen diffusion data are reproduced in Figure 5.

Finally other work concerned with the optimal electrode geometry has described some dramatic differences in apparent power density depending on the area ratio of the cathode:anode (98). When non-symmetrical cells are used in determination of the materials performance, an enhancement of up to three times that of the symmetrical cell was reported. This highlights the need for accurate details of experimental configuration, and indeed careful comparison of the data obtained from groups using different methodologies.

MATERIALS FOR PEMFC STACKS

A key issue influencing materials developments for PEMFCs is that of materials cost. Table 1 presents some recently published cost data for a PEMFC stack (99).

Such cost estimates are necessarily speculative owing to the early stage of the technology, but they do indicate the prime targets for materials research. Therefore, it is clear that if projected cost estimates for PEMFC systems of around 50 kWe rating are to reach recent estimates of 40–200 US$/kWe (100, 101) (based on production volumes of at least 30,000 units per annum, and including fuel cell stack, auxiliary systems, and power electronics, but not fuel storage), materials development needs to focus on the key areas of bipolar plates, electrocatalysts, and membranes, always taking into account the need to be able to manufacture large numbers of these components in a cost-effective manner. Further discussion of the costs of PEMFC stacks and systems are found below.

Bipolar Plates

Early bipolar plates in PEMFCs were made of machined graphite. This is not a technologically viable option owing to both cost and weight considerations, with the result that other materials are under development, primarily metals and carbon-polymer composites.

Cost estimates of PEMFCs produced using stainless steel bipolar plates suggest that a 70-kWe stack costing less than US$20/kWe can be achieved (102). Frequently, 316 stainless steel has been the alloy of choice for metallic bipolar plates. However, a number of alternative grades of stainless steel have now been

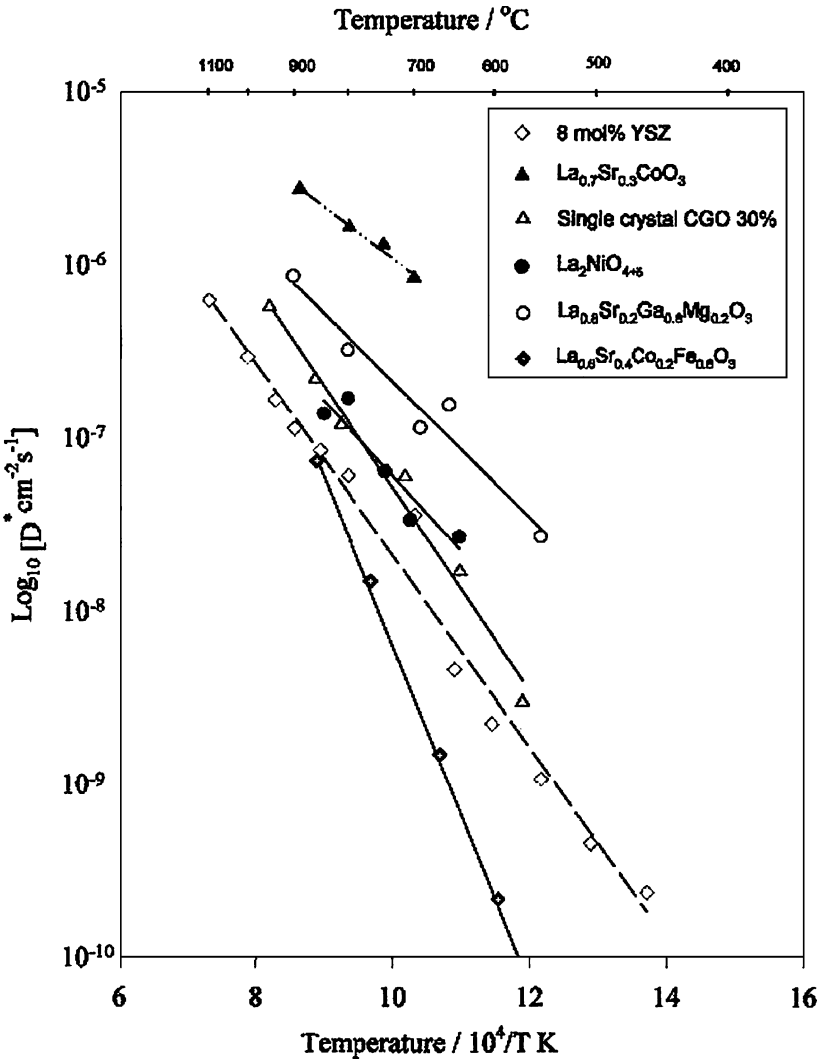

Figure 5 Oxygen self-diffusion coefficients of selected cathode and electrolyte materials.

evaluated in terms of the electrical resistance of their surface oxide film (103, 104). These studies suggest that because of the formation of an oxide layer with high resistivity and poisoning of the membrane electrode assembly (MEA) by corrosion products, the use of stainless steel is only possible with protective coatings. Examples of coatings include a gold electrocoat (105), although cost is clearly an issue here, and a carbon-based film obtained by pyrolyzing a high carbon-content polymer sprayed on the surface of the steel (106). Hodgson et al. (107) have shown

TABLE 1 Cost data for a PEMFC stack

Material	Cost US$/kW$_e$
Bipolar plate	825
Electrocatalyst	243
Membrane	120
Electrode	31
End plate	0.24
Plastic frame	0.11
Total	1220

that coated titanium can also be employed to produce fuel cells with very high volumetric and gravimetric power densities.

In the case of carbon-polymer composites, the great majority of these materials involve the hot molding of a carbon or graphite filler in a thermosetting or thermoplastic matrix. There is a trade-off between mechanical strength and electrical conductivity. Some typical conductivity values are $\sim$1000 S m^{-1} for polymer/graphite materials, well above that of the membrane, though still below the conductivity values of 5.3×10^8 S m^{-1} for iron-based alloys and 2.4×10^8 S m^{-1} for titanium. Usually, conductivities lower than that of graphite are reported for the molded plates. This lowers the power density of the stack. For example, Del Rio et al. (108) report the use of PVDF, incorporating varying amounts of carbon black. Conductivity results indicate that these materials possess an electronic conductivity up to 24 S m^{-1}, which diminishes slightly with increasing temperature. Carbon-carbon composite plates are also under development (109).

Electrocatalysts

A catalytically active layer sits adjacent to the electrolyte membrane within both the anode and cathode of a PEMFC. The layer is supported on a PTFE-treated carbon paper, which acts as a current collector and gas diffusion layer, thus enabling the transport of gas, water, and electrons. For operation with pure hydrogen and air, platinum is the most active electrocatalyst. To reduce cost, nano-particles of platinum on a carbon support have been developed, and ongoing development of stable nano-structures continues to be an important aspect of fuel cell development (110).

However, a key aspect of electrocatalyst development relates to the development of anode catalysts for operation on reformed hydrogen from methanol, natural gas, or gasoline. This is because, while gas-diffusion electrodes with a loading of 0.1 to 0.2 mg cm^{-2} of dispersed platinum on carbon show very small polarization losses when operating on pure H_2, these losses are raised to unacceptable values when even small amounts of CO are present (100 ppm for example), as is always

the case in reformate mixtures. Using a large variety of experimental approaches, many attempts have been made to understand the mechanism of CO poisoning. It is generally proposed that CO poisoning occurs because of a strong adsorption of CO on the catalyst surface that blocks the hydrogen adsorption step.

There are three main strategies to overcome the CO poisoning problem in PEMFCs. The first is to bleed very low levels of oxidant, such as oxygen, into the fuel stream post reforming. This oxidizes the CO through to CO_2, at the expense of some fuel loss and increased system cost. This pragmatic approach is the one presently adopted by many fuel cell developers. The second approach is to operate the PEMFC at higher temperatures, which helps suppress the adverse impact of CO. However, this requires the development of new high-temperature membranes, in itself a significant materials challenge, and one discussed in detail below.

Of relevance here is the third approach of developing new CO-tolerant electrocatalysts. Most work in this area has concentrated on Pt-M (where M is usually a transition metal) bimetallic catalysts (111–116). Some success has been reported using high-energy milling of Pt, Pt-Ru (117), and Pt-Mo (118) catalysts. Igarashi et al. (111) have reported new CO-tolerant catalysts by alloying Pt with a second non-precious metal, so as to reduce cost, and Pt-Fe, Pt-Ni, Pt-Co, and Pt-Mo alloys were reported to exhibit excellent CO tolerance in H_2 oxidation, similar to that of the Pt-Ru alloy. Haug et al. (113) placed a layer of carbon-supported Ru between the Pt catalyst and the anode flow field to promote the conversion of adsorbed CO to CO_2. Escudero et al. (114) have prepared electrocatalysts based on Pt, Pt-Ru, and Pt-Pd by microemulsion methods, which allows the production of a very narrow size distribution of metal particles, with an average size smaller than that of conventional electrocatalysts prepared by impregnation.

Recent work on cathode electrocatalysts has largely focused on understanding the mechanism of oxygen reduction on Pt-based bimetallic catalysts, for example Pt-Fe (119), Pt-Ni, and Pt-Co (120).

Electrolyte Membranes

Proton-conducting membranes form the core of PEMFCs. The following membrane properties need to be optimized for fuel cell applications: (*a*) fast proton transport; (*b*) good mechanical, chemical, and thermal properties requiring the selection of a suitable polymer backbone, and possibly membrane reinforcement; (*c*) low gas permeability; and (*d*) low levels of swelling.

There is significant interaction between these properties and the type of backbone polymer and the degree of sulfonation and nano-phase separation into hydrophilic and hydrophobic domains (for example, high levels of sulfonation typically lead to high conductivity but also to a high level of swelling). A number of materials are under consideration in an attempt to meet these conflicting requirements.

Classically, Nafion^{TM} type perfluorinated polymer membranes, which have a PTFE-like backbone and relatively low equivalent weight, are used as the electrolyte. However, the cost of these materials remains high [around US\$56 m^{-2}

in large volumes (101)]. Furthermore, the lack of selectivity for methanol of these membranes, when considering the development of direct methanol cells for example, combined with the problem of recycling fluorinated polymers (121), are all additional reasons for the development of new electrolyte membranes. This need is all the more crucial if the target of increasing the temperature of operation to 150 to 200°C (in order to minimize the problem of poisoning of the catalysts from carbon monoxide) is to be realized. The upper temperature limit of operation of Nafion is generally regarded to lie around 140°C.

Micro-reinforced composite membranes that consist of a microporous stretched PTFE membrane whose pores are filled with perfluorinated ionomer have also been developed. The membrane is mechanically stabilized by the PTFE host so that membrane thickness can be reduced, leading to a decreased resistance to proton transport.

Considerable effort is being applied to the development of lower cost, usually fluorine free, hydrocarbon-based membrane materials. These offer a number of potential advantages: (*a*) They are cheaper than perfluorinated ionomers, and many kinds of materials are commercially available; (*b*) they contain polar groups that have a high water uptake over a wide temperature range, and the absorbed water is restricted to the polar groups of polymer chains; (*c*) decomposition of hydrocarbon polymers can be depressed to some extent by proper molecular design; and (*d*) they are more readily recycled by conventional methods.

Because hydrocarbon membranes often suffer from insufficient thermal stability, additional aromatic groups are introduced into the polymer backbone. However, concern remains about the long-term stability of membranes based on these materials, which to date remains unproven. The following summarizes recently reported studies on alternative polymer electrolyte materials.

Membranes based on polybenzimidazole (PBI), which forms adducts with inorganic acids, are candidate materials for high-temperature applications and have been the subject of much recent interest (122–130). These membranes exhibit high conductivities at relatively low humidity compared with conventional low-temperature membranes. PBI exhibits good thermochemical stability and mechanical properties. It is cheaper and has much lower permeability for hydrogen than Nafion.

Jones & Roziere (122) have recently reviewed work on the functionalization by acid doping, chemical grafting of protogenic groups, or direct sulfonation by electrophilic substitution on the polymer backbone of both polybenzimidazole and polyetherketones with a view to increasing their proton conductivity without detriment to their thermohydrolytic and chemical stability. It was shown that a considerable increase in proton conductivity could be achieved by these means, partly owing to an increase in the density of mobile protons, but also to increased water uptake arising from the presence of protogenic groups. It was also shown, however, that the degree of functionalization must be carefully controlled because the enhanced hydrophilicity can lead to increased softness of the polymer, irreversible swelling, and, in extreme cases, water solubility. When operating within these

constraints, the proton conductivity of phosphoric acid–complexed PBI, base-doped benzylsulfonate-grafted PBI, and sulfonated polyetherketone was shown to reach around 1 S m^{-1} at the fuel cell operating temperature.

Staiti et al. (124) prepared composite membranes based on phosphotungstic acid (PWA) adsorbed on silica and PBI. Membranes with high tensile strength and thickness of less than 30 μm could be cast. They were chemically stable in boiling water and thermally stable in air up to 400°C. A maximum conductivity of 0.3 S m^{-1} was obtained at 100% relative humidity and 100°C, with membranes containing 60 wt% PWA/SiO_2 in PBI. Conductivity measurements performed at higher temperatures, in the range of 90 to 150°C, gave almost stable values of 0.15 S m^{-1} at 100% relative humidity.

Inorganic/organic composite membranes formed by polybenzimidazole, silicotungstic acid, and silica with different ratio between them have also been prepared and characterized before and after treatment in phosphoric acid (130). Silica behaved as a support on which the heteropolyacid remained blocked in a finely dispersed state and as an adsorbent for water, enhancing proton conduction. The membrane with 50 wt% of SiWA-SiO_2/PBI had a proton conductivity of 0.12 S m^{-1} at 160°C and 100% relative humidity. After treatment with phosphoric acid the proton conductivity of membranes increased to 0.22 S m^{-1}.

Lopez et al. (131) prepared cation-exchange membranes from polymer composites based on polyvinylidene fluoride (PVDF), sulfonated polystyrene-co-divinylbenzene (PS-co-DVB), and antimonic acid. Genova-Dimitrova et al. (132) prepared ionomeric membranes for PEMFCs composed of sulfonated polysulfone (SPSF) associated with phosphato-antimonic acid. These composite membranes provided conductivities close to Nafion membranes, while avoiding dissolution or excessive water swelling at 80°C. However, proton conductivity in sulfonated polymer materials relies on proton solvation by water at high water activities, in which case this class of materials suffers temperature limitations similar to those of Nafion.

Modification of sulfonated membranes by the inclusion of small inorganic particles such as silica (122, 133, 134, 136, 137) or zirconium phosphates (138) leads to an improvement in performance at higher temperatures. Also the morphological stabilization of acidic polymers by either acid/base blending or covalent cross linking (139–141) appears to reduce swelling and water cross-over. However, problems of relatively low conductivity and brittleness in the dry state can occur (142).

A series of composite membranes based on sulfonated polyether ketone (SPEEK) with embedded powdered heteropolycompounds (HPA) has been reported (143). The HPAs used were tungsto-phosphoric acid, $H_3PW_{12}O_{40}$, 29 H_2O (TPA), molybdo-phosphoric acid, $H_3PMo_{12}O_{40}$, 29 H_2O (MPA), and the di-sodium salt of tungsto-phosphoric acid, $Na_2HPW_{12}O_{40}$ (Na-TPA). The conductivity of the composite membranes exceeded 1 S m^{-1} at room temperature, and around 10 S m^{-1} above 100°C.

Kreuer (142) has recently presented two approaches toward producing higher temperature membranes. The first is based on the modification of the microstructure

of sulfonated polyaryls (such as polyetherketones functionalized by electrophilic sulfonation with sulfuric acid) by blending with other polymers. Water cross-over can be significantly reduced while maintaining high proton conductivity, which is particularly important in direct methanol PEMFCs. In a second approach, Kreuer presents preliminary results for a fully polymeric proton-conducting membrane, with no volatile proton-conducting solvent (such as water). This offers the prospect of operation at temperatures significantly beyond 100°C and is based on oligomers consisting of short polyethylene oxide terminated by imidazole groups.

Sol-gel derived Nafion/silica hybrid membranes have been investigated by Miyake et al. (144). Membrane proton conductivity and water content were measured as a function of temperature, water vapor activity, and silica content. The hybrid membranes had a higher water content at 25 and 120°C, but not at 150 and 170°C. Despite the higher water content, the proton conductivities in the hybrid membranes were no greater than that in unmodified Nafion membranes under all conditions investigated.

Doyle et al. (145) demonstrated that perfluorinated ionomer membranes, such as Nafion, can be swollen with ionic liquids, giving composite free-standing membranes with excellent stability and proton conductivity in this temperature range while retaining the low volatility of the ionic liquid. Ionic conductivities in excess of 10 S m^{-1} at 180°C have been demonstrated using the ionic liquid 1-butyl, 3-methyl imidazolium trifluoromethane sulfonate.

Highly proton-conducting organic-inorganic glass hybrids have been prepared using the sol-gel method, the electrical conductivities of which were studied in relation to their thermal and mechanical properties (146). A solution of hydrolyzed $Si(OC_2H_5)_4$ and H_3PO_4 was reacted with a perfluorosulfonic polymer such as Nafion, forming a homogeneous hybrid-gel. The conductivity of the hybrid-gel incorporated with 20% Nafion was $\sim$1 S m^{-1} at room temperature, reaching around 6 S m^{-1} at 200°C.

A novel method for the preparation of a self-humidifying membrane used for a polymer electrolyte membrane fuel cell has been presented by Yang et al. (147). Generation of water molecules on the Pt particles embedded in the membrane by the recombination of permeated hydrogen and oxygen was attributed to the higher performance of a single cell prepared using the self-humidifying membrane.

Sol-gel processes have been used by Nakajima et al. (148) to synthesize polymer electrolyte membranes consisting of organic/inorganic nano-hybrid macromolecules by cross-linking nano-sized silicate species to polyether polymers, polyethylene oxides, polypropylene oxide, and polytetramethylene oxide, and doping with heteropolyacids such as 1,2-phosphotungstic acid. Conductivities of approximately 1 S m^{-1} at 140°C under humidified conditions were reported.

Projected Costs of PEMFC Materials and Systems

A.D. Little (101) recently projected the manufacturing costs of PEMFC systems, taking the case of 500,000 units per year of a 50-kWe net system. The materials used for the analysis are indicative of current industrial thinking regarding state-of-the-art materials in this area. The 20-μm-thick cathode catalyst layer

contained a precious metal loading of 0.4 mg Pt cm^{-2}, the 20-μm-thick anode catalyst layer a loading of 0.2 mg Pt cm^{-2} and 0.4 mg Ru cm^{-2}. The gas diffusion layers, which back onto the catalyst layers, were 100-μm-thick PTFE-treated carbon paper. The electrolyte was a 40-μm-thick perfluorosulfonic acid membrane operating at a temperature of 80°C on reformed gasoline containing 100 ppm CO. The bipolar plate was manufactured from a high-purity graphite/vinyl ester composite, 4.75 mm thick, with integral cooling channels, manufactured in two pieces before bonding. The stack operated at a relatively high cell voltage of 0.8 V to increase stack efficiency to 54%, and system efficiency to 37%, but at the expense of a relatively low-power density of 0.25 W cm^{-2}.

On this basis, the study gives some indication of the costs achievable with volume manufacture. Of a total system cost of around US$300 k We^{-1}, excluding fuel storage, 60% was attributed to the fuel cell stack, 29% to the fuel processor, 8% to assembly and indirect costs, and 3% to balance of plant. In total, materials costs were predicted to make up a significant 81% of the total system cost, showing that advances in materials are vital if component size, weight, and cost is to be reduced further. Table 2 indicates the breakdown of the materials costs in more detail, showing that whereas the MEA dominates the cost of the fuel cell, the cost of other components remains significant.

Table 3 presents a more detailed analysis of the costs and weight of the materials used within the MEA and bipolar plates. The MEA itself was predicted to cost US$236 m^{-2}, with the cost of materials dominating over the cost of manufacturing. This is a clear indication that materials costs must be reduced, for example, by the

TABLE 2 Distribution of materials costs (101) for a 50-kWe PEMFC system at 500,000 units per annum (total materials cost around US$12,000 per 50-kWe unit)

Component	Breakdown by materials cost (%)
MEA	45
Bipolar plates	7
Balance of stack	3
Fuel processing catalysts	10
Stainless steel	7
Valves	8
Radiators	6
Sensors	5
Compressors/expanders	4
Pumps and motors	3
Circuit boards and wiring	2

TABLE 3 MEA and bipolar plate materials and processing costs and weight for a 50-kWe PEMFC system at 500,000 units per annum (101)

	Material	Material cost US$ m^{-2}	Processing cost US$ m^{-2}	Total cost US$ m^{-2}	Weight kg m^{-2}	Total cost US$ kWe^{-1}
MEA	Anode GDL	8.81	0.48	9.29	0.21	4
	Anode CL	80.58	2.11	82.69	0.02	38
	Electrolyte	56.13	1.78	57.91	0.08	26
	Cathode CL	75.20	1.98	77.18	0.02	35
	Cathode GDL	8.81	0.48	9.29	0.21	4
MEA Total		229.51	6.84	236.35	0.54	107
Bipolar plate		37.19	8.48	45.67	5.84	21

CL = catalyst layer, GDL = gas diffusion layer

successful development of low-cost electrolyte membranes. The development of high-temperature electrolyte membranes will also have an impact on cost, as they will be able to simplify the fuel processor, which comprises a significant 29% of the system cost. Fuel processor costs are considered in more detail below.

MATERIALS FOR REFORMERS

Reformers for PEMFCs

The relatively low-operating temperature of PEMFCs means that fuel processing is carried out in an external reformer. The wide range of potential applications of this technology also means that a wide range of fuel types need to be processed into clean hydrogen containing only a few ppm CO. Fuels of interest include natural gas, methanol, diesel, and low sulfur gasoline. Also of importance is the need to produce compact, lightweight, and low-cost reformers. This imposes considerable challenges on the reformer subsystem for PEMFCs. Key areas for materials development relate to the development of catalysts for reforming many fuels and the engineering challenges of developing compact reformers. A review of reforming strategies and thermodynamics can be found in, for example, the recent paper by Ahmed & Krumpelt (149).

Joensen & Rostrup-Nielsen recently reviewed the conversion of hydrocarbon and alcohol fuels for SOFCs and PEMFCs (150). The authors suggest that, while new palladium catalysts have been reported for methanol reforming for PEMFCs, conventional copper-based catalysts continue to be preferred on the basis of cost.

Another recent review of catalysts for PEMFC fuel reforming has been produced by Urban et al. (151). Again, CuO-ZnO on Al_2O_3 was identified as the standard catalyst for the steam reforming of methanol. Pt/Al_2O_3 catalysts have also been reported for the partial oxidation of methanol (152).

Hydrocarbons are more difficult to reform than methanol, requiring substantially higher temperatures and more steam or air to avoid carbon formation. Urban

et al. (151) have summarized the turnover frequency of different metals for the steam reforming of ethane and methane, normalized to that of nickel, which is the conventional catalyst used in stationary applications of steam reforming. For both fuels, turnover frequency increased in the order Rh > Ru > Ni > Pd > Pt. Thus for mobile or portable applications, more expensive noble metal catalysts may be preferred because smaller catalyst volumes are needed.

Another important component in reformers for PEMFCs is the need for a shift catalyst to reduce the CO content. This involves a high-temperature (350–400°C) shift reactor using Fe/Cr oxide catalysts. This is followed by a low-temperature (180–250°C) shift reactor, using Cu/Zn oxide catalysts. New catalyst developments are focusing on precious metal-based catalysts (153, 154) for these reactors, which are less prone to the problems of sulfur sensitivity and also deactivation via oxidation during cold start conditions.

Another approach to reducing reformer size and weight is increased thermal integration and miniaturization via engineering development. Although outside the scope of this review, an example is given in the work of Nagano (155) who reports improved heat transfer in methanol steam reforming via the use of internal corrugated heat exchangers.

The reformer sub-system can be a significant cost element of the overall PEMFC system. A recent report by A.D. Little (101) on a 50-kWe fuelled PEMFC system capable of operating on gasoline indicated that the fuel processor sub-system made up 29% of the system cost (on the basis of 500,000 units per annum, and excluding fuel storage costs) and 35% of the weight. The report assumes a fuel processor sub-system incorporating an autothermal reformer with a Pt/Ni catalyst operating at 1030°C, a high-temperature shift reactor with an Fe_3O_4/CrO_3 catalyst operating at 430°C, a low-temperature shift reactor with a Cu/ZnO catalyst operating at 230°C, and a partial oxidation reformer with a Pt catalyst operating at 205°C. ZnO and activated carbon are incorporated to remove sulfur and ammonia, respectively. A Pt catalyst is also incorporated into the off-gas burner, resulting in 14% of the total precious metal content of the PEMFC system being located within the fuel processing sub-system. The report concludes that the performance, cost, and robustness of the fuel processor catalysts are critical to the size and cost of the fuel processor.

Materials for Advanced Reformers for SOFCs

Dicks (156, 157) has reviewed the options for reforming natural gas for high-temperature fuel cells, including SOFCs. The challenges facing SOFC reforming differ considerably from those for PEMFCs. For example, for SOFCs the fuel of interest is usually natural gas. The high temperature of operation of SOFCs enables internal reforming to be used, typically using nickel catalysts, where the waste heat from the fuel cell reaction can be used to drive the endothermic steam-reforming reaction. In this embodiment, the reformer is contained within the stack core, and indeed reforming may be carried out directly on the fuel cell anodes. This presents other challenges, namely the rapid kinetics of the endothermic reforming reaction inducing local cooling of the fuel cell and hence cracking of the delicate ceramic components. This process has been modeled in recent work by Aguiar et al. (158),

who showed that the use of typical metal (Ni)-based steam reforming catalysts leads to undesirable local cooling owing to the mismatch of the local reforming rate with the heat available from the fuel cell.

Recent materials developments in this area have therefore focused on developing catalyst structures that control the reforming rate. For example, the use of diffusion barriers of ceria or zirconia around conventional Ni-reforming catalysts, applied using sols, is an effective strategy to reduce the rate of the reforming reaction, while the catalyst performance is maintained in the face of possible deactivation over time (159).

Another important aspect of fuel processing within SOFCs relates to the development of new anode materials that are capable of directly oxidizing fuel gases such as methane or tolerant of the direct reforming process within the anode structure. This is a topical research area in the field and is covered within this volume by Mogensen & Kammer (45a).

CONCLUDING REMARKS

Alternative stack configurations such as the single-chamber mixed reactant and compact flow-through mixed reactant designs continue to be proposed (160). Likewise, theoretical analyses have suggested PEMFC/SOFC combinations (161) and cascaded SOFC stacks (162) to increase system efficiencies. However, in the next decade it is likely that much research and development will focus on reducing processing costs of existing stack materials and increasing the durability of available components.

Fortunately, innovative materials engineers can still have a major impact on the commercialization of fuel cell technology. The challenge is to design, and process economically, materials that would allow PEMFC stacks and associated reformers to operate at elevated temperatures (150–200°C), IT-SOFC systems to operate at 500–700°C with improved oxide anodes to allow direct reforming of hydrocarbon fuels, and battery replacement fuel cells for portable electronic devices (163). Materials engineers have the opportunity to overcome these challenges and to ensure that fuel cells become a commercial success rather than a perennial promising future technology.

The *Annual Review of Materials Research* is online at http://matsci.annualreviews.org

LITERATURE CITED

1. Appleby AJ, Foulkes FR. 1989. *Fuel Cell Handbook*. New York: Van Nostrand Reinhold
2. Blomen LJN, Mugerwa MN, eds. 1993. *Fuel Cell Systems.* New York: Plenum
3. Kordesch KV, Simader G. 1996. *Fuel Cells and Their Applications*. Weinheim: VCH
4. Larminie J, Dicks AL. 2000. *Fuel Cell Systems Explained*. New York: Wiley

5. Kordesch KV. 1978. *J. Electrochem. Soc.* 125:77C–91C
6. Appleby AJ. 1990. *J. Power Sources* 29:3–11
7. *Fuel Cell Handbook.* 2002. Morgantown, PA: US Dept. Energy. 6th. ed.
8. Grove VII. 2002. *J. Power Sources* 106:1–411

8a. *Fuel Cells Bulletin, Monthly International Newsletter.* Oxford, UK: Elsevier ISSN 1464-2859

9. MacKerron G. 2000. *J. Power Sources* 86:28–33
10. Surdoval WA, Singhal SC, McVay GL. 2001. In *Proc. SOFC VII*, Proc. Vol. 2001-16, ed. H Yokokawa, SC Singhal, pp. 53–62. Pennington, NJ: Electrochem. Soc.
11. Jeong K, Oh B. 2002. *J. Power Sources* 105:58–65
12. Hartvigsen J, Khandkar A, Elangovan S. 1999. In *Proc. SOFC VI*, Proc. Vol. 99-19, ed. SC Singhal, M Dokiya, pp. 1135–41. Pennington, NJ: Electrochem. Soc
13. Steele BCH, Heinzel A. 2001. *Nature* 414:345–52
14. Schlapbach L, Zutell A. 2001. *Nature* 414:353–58
15. Wang SZ, Ishihara T, Takita Y. 2002. *Electrochem. Solid State Lett.* 5:A177–80
16. Dicks AL, Larminie J. 2000. *Reforming of fossil fuels.* Presented at Proc. Fuel Cell 2000. Ed. L Blomen, pp. 57–67. Oberrohrdorf, Switzerland: Eur. Fuel Cell Forum
17. Bae J-M, Steele BCH. 1998. *Solid State Ionics* 106:247–53
18. Morgensen M, Jensen KV, Jorgensen MJ, Primdahl S. 2002. *Solid State Ionics* 150:123–29
19. de Ridder M, van Welzenis RG, Brongersma HH, Wulff S, Chu WF, Weppner W. 2002. *Phys. Res. B* 190:732–35
20. Kawada T, Yokokawa H. 1997. *Key Eng. Mater.* 125–126:187–248
21. Badwal SPS. 2001. *Solid State Ionics* 143:39–46
22. Steele BCH. 2001. *J. Mater. Sci.* 36:1053–68
23. Tietz F, Buchkremer H-P, Stover D. 2002. *Solid State Ionics* 152–53:373–81
24. Will J, Mitterdorfer A, Kleinlogel C, Perednis D, Gauckler LJ. 2000. *Solid State Ionics* 131:79–96
25. Gardner FJ, Day MJ, Brandon NP, Pashley MN, Cassidy M. 2000. *J. Power Sources* 86:122–29
26. Sverdrup EF, Warde CJ, Eback RL. 1973. *Energy Conversion* 13:129–41
27. Report. Institute of High Temperature Electrochemistry, Ekatrinburg, Russia
28. Kendall K, Sales G. 1994. *Ceram. Energy Appl. II*, pp. 55–63. London: Institute of Energy
29. Tompsett GA, Brown MS, Finnerty C, Sammes NM, Kendall K. 2000. *Design of a tubular micro-SOFC demonstration system.* Presented at Eur. SOFC Forum, ed. AJ McEvoy, pp. 13–18. Oberrohrdorf, Switzerland: Eur. Fuel Cell Forum
30. Tedman CS, Spacil HS, Mitoff SP. 1969. *J. Electrochem. Soc.* 116:1170–75
31. Piron-Abellan J, Tietz F, Shemet V, Gil A, Ladwein T, et al. 2002. *Long term oxidation behavior and compatibility with contact materials of newly developed ferritic interconnector steel.* Presented at 5th Eur. SOFC Forum, pp. 248–53. Oberrohrdorf, Switzerland: Eur. Fuel Cell Forum
32. Uehara T, Ohno T, Toji A. 2002. *Development of ferritic Fe-C_4 alloy for a SOFC separator.* Presented at 5th Eur. SOFC Forum, pp. 281–88. Oberrohrdorf, Switzerland: Eur. Fuel Cell Forum
33. Honegger K, Diethelm R, Glatz W. 2001. In *SOFC VII*, Proc. Vol. 2001-16, ed. H Yokokawa, SC Singhal, pp. 803–10. New Jersey: Electrochem. Soc
34. Gindorf C, Hilpert K, Singheiser L. 2001. In *Proc. SOFC VII*, Proc. Vol. 2001-16, ed. H Yokokawa, SC Singhal, pp. 793–802. New Jersey: Electrochem. Soc.
35. Batawi E, Plas A, Staub W, Honegger K, Diethelm R. 1999. In *Proc. SOFC VI*, Proc. Vol. 99-19, ed. SC Singhal, M Dokiya, pp. 767–73. New Jersey: Electrochem. Soc

36. Ghosh D. 2002. *Development of stationary solid oxide fuel cells.* Presented at 5th Eur. SOFC Forum, pp. 453–59. Oberrohrdorf, Switzerland: Eur. Fuel Cell Forum
37. Minh N, Anumakonda A, Doshi R, Guan J, Huss S, et al. 2001. In *Proc. SOFC VII*, Proc. Vol. 2001-16, ed. H Yokokawa, SC Singhal, pp. 190–95. New Jersey: Electrochem. Soc
38. Lang M, Henne R, Metzger P, Schiller G. 2002. *Vacuum plasma spraying of thin film planar SOFF: development status at DLR Stuttgart.* Presented at 5th Eur. SOFC Forum, pp. 10–17. Oberrohrdorf, Switzerland: Eur. Fuel Cell Forum
39. Visco S, Jacobson CP, De Jonghe LC. 2001. In *Ionic and Mixed Conducing Ceramics IV*, Proc. Vol. 2001-28, pp. 368–73. New Jersey: Electrochem. Soc
40. Steele BCH. 2000. *Solid State Ionics* 129:95–11

40a. Oishi N, Rudkin R, Brandon NP, Lewis G, McColm T, Steele BCH. 2002. *Operation at 500–600°C of stainless steel supported thick film.* Presented at 2002 Fuel Cell Seminar Abstracts, Palm Springs, CA. pp. 1–4 (CD version)

41. Majewski P, Rozumek M, Tas CA, Aldinger F. 2002. *J. Electroceram.* 8:65–73
42. Meng GY, Fu QX, Zha SW, Xia CR, Liu XQ, Peng DK. 2002. *Solid State Ionics* 148:533–37

42a. Goodenough JB. 2003. *Annu. Rev. Mater. Res.* 33:91–128

43. Marisnek M, Zupan K, Maeek J. 2002. *J. Power Sources* 106:178–88
44. Ringuede A, Bronine D, Frade JR. 2002. *Solid State Ionics* 146:219–24
45. Fukui T, Ohara S, Murata K, Yoshida H, Miura K, Inagaki T. 2002. *J. Power Sources* 106:142–45

45a. Mogensen M, Kammer K. 2003. *Annu. Rev. Mater. Res.* 33:321–31

46. Kim H, Lu C, Worrell WL, Vohs JM, Gorte RJ. 2002. *J. Electrochem. Soc.* 149:A247–50
47. McEvoy AJ. 2002. *Mater. Werkstofftech.* 33:331–34
48. Hibino T, Hashimoto A, Yano M, Susuki M, Yoshido S, Sano M. 2002. *J. Electrochem Soc.* 149:A133–36
49. Huang K, Wan JH, Goodenough JB. 2001. *J. Electrochem. Soc.* 148:A788–94
50. Lu Z, Pei L, He T-M, Huang X-Q, Liu Z-G. 2002. *J. Alloys Compounds* 334:299–303
51. Carter D. 2002. *MRS Bull.* 27:490
52. Hui SQ, Petric A. 2002. *J. Eur. Ceram. Soc.* 22:1673–81
53. Kharton VV, Figueiredo FM, Navarro L, Naumovich EN, Kovalevsky AV, et al. 2001. *J. Mater. Sci.* 36:1105–17
54. Liu J, Madsen BD, Ji ZQ, Barnett SA. 2002. *Electrochem. Solid State Lett.* 5: A122–24
55. Primdahl S, Hansen JR, Grahl-Madsen L, Larsen PH. 2001. *J. Electrochem. Soc.* 148:A74–81
56. Stormer AO, Holtappels P, Tu HY, Stimming U. 2002. *Mater. Werkstofftech.* 33: 339–42
57. Vashook V, Muller R, Zosel J, Ahlborn K, Ullmann H, Guth U. 2002. *Mater. Werkstofftech.* 33:335–38
58. Vazquez JC, Zhou W, Irvine JTS. 2001. In *Electron Microscopy and Analysis. Ser. 168*, pp. 295–98. Bristol, UK: Inst. Physics Conf.
59. Vernoux P, Djurado E, Guillodo M. 2001. *J. Am. Ceram. Soc.* 84:2289–95
60. Wang S, Kato T, Nagata S, Honda T, Kaneko T, et al. 2002. *J. Electrochem. Soc.* 149:A927–33
61. Wang S, Kato T, Nagata S, Honda T, Kaneko T, et al. 2002. *Electrochemistry* 70:252–57
62. Marina OA, Pederson LR. 2002. Presented at 5th Eur. SOFC Forum, pp. 481–89. Oberrohrdorf, Switzerland: Eur. Fuel Cell Forum
63. Kunifusa Y, Yoshinaka M, Hirota K, Yamaguchi O. 2002. *Solid State Ionics* 149:107–13
64. Sauvet AL, Fouletier J, Gaillard F, Primet M. 2002. *J. Catalysis* 209:25–34

65. Skinner SJ. 2001. *Int. J. Inorg. Mater.* 3: 113–21
66. Hart NT, Brandon NP, Day MJ, Lapena-Rey N. 2002. *J. Power Sources* 106:42–50
67. Hart NT, Brandon NP, Day MJ, Shemilt JE. 2001. *J. Mater. Sci.* 36:1077–85
68. Holtappels P, Bagger C. 2002. *J. Eur. Ceram. Soc.* 22:41–48
69. Xia C, Rauch W, Wellborn W, Liu M. 2002. *Electrochem. Solid State Lett.* 5:A217–20
70. Yoon SP, Han J, Nam SW, Lim TH, Oh IH, et al. 2002. *J. Power Sources* 106:160–66
71. Gaudon M, Laberty-Robert C, Ansart F, Stevens P, Rousset A. 2002. *Solid State Sci.* 4:125–33
72. Horita T, Yamaji K, Sakai N, Yokokawa H, Weber A, Ivers-Tiffee E. 2001. *J. Electrochem. Soc.* 148:A456–62
73. Simner SP, Bonnett JF, Canfield NL, Meinhardt KD, Sprenkle VL, Stevenson JW. 2002. *Electrochem. Solid State Lett.* 5:A173–75
74. Dasgupta N, Krishnamoorthy R, Jacob KT. 2002. *Mater. Sci. Eng. B* 90:278–86
75. Dasgupta N, Krishnamoorthy R, Jacob KT. 2002. *Solid State Ionics* 149:227–36
76. Tu HY, Takeda Y, Imanishi N, Yamamoto O. 1999. *Solid State Ionics* 117:277–81
77. Ishihara T, Fukui S, Nishiguchi H, Takita Y. 2002. *J. Electrochem. Soc.* 149: 823–28
78. Lu X, Liu M. 2002. *Solid State Ionics* 149:299–307
79. Kharton VV, Shaulo AL, Viskup AP, Avdeev M, Yaremchenko AA, et al. 2002. *Solid State Ionics* 150:229–43
80. Kharton VV, Yaremchenko AA, Viskup AP, Patrakeev MV, Leonidov IA, et al. 2002. *J. Electrochem. Soc.* 149:E125–35
81. Patrakeev MV, Mitberg EB, Lakhtin AA, Leonidov IA, Kozhevnikov VL, et al. 2002. *J. Solid State Chem.* 167:203–13
82. Chinarro E, Colomer MT, Jurado JR. 2002. *Key Eng. Mater.* 206-2:151–54
83. Colomer MT, Chinarro E, Jurado JR. 2002. *Key Eng. Mater.* 206-2:155–58
84. Bassat JM, Boehm E, Grenier JC, Mauvy F, Dordor P, Pouchard M. 2002. *YSZ supported cathodes of rare earth nucleates $La_2NiO_{4-\delta}$ for IT-SOFC (650°C).* Presented at 5th Eur. SOFC Forum, pp. 586–93. Oberrohrdorf, Switzerland: Eur. Fuel Cell Forum
85. Vashook VV, Tolochko SP, Yushkevich II, Makhnach LV, Kononyuk IF, et al. 1988. *Solid State Ionics* 110:245–53
86. Skinner SJ, Kilner JA. 1999. *Ionics* 5:171–75
87. Skinner SJ, Kilner JA. 2000. *Solid State Ionics* 135:709–12
88. Kharton VV, Viskup AP, Naumovich EN, Marques FMB. 1999. *J. Mater. Chem.* 9:2623–29
89. Kharton VV, Viskup AP, Naumovich EN, Marques FMB. 1999. *Solid State Ionics* 146:203–10
90. Xia CR, Liu ML. 2002. *Adv. Mater.* 14: 521–23
91. Barbucci A, Bozzo R, Cerisola G, Costamagna P. 2002. *Electrochim. Acta* 47:2183–88
92. Wang S, Kato T, Nagata S, Honda T, Kaneko T, et al. 2002. *Solid State Ionics* 146:203–10
93. Perry-Murray E, Sever MJ, Barnett SA. 2002. *Solid State Ionics* 148:27–34
94. Fukui T, Ohara S, Naito M, Nogi K. 2001. *J. Nanoparticle Res.* 3:171–74
95. Dusastre V, Kilner JA. 1999. *Solid State Ionics* 126:163–74
96. Adler SB, Lane JA, Steele BCH. 1996. *J. Electrochem. Soc.* 143:3554–64
97. Adler SB. 2000. *Solid State Ionics* 135: 603–12
98. Chung BW, Pham AQ, Haslam JJ, Glass RS. 2002. *J. Electrochem. Soc.* 149:A325–30
99. Jeong K, Oh B. 2002. *J. Power Sources* 105:58–65
100. Lomax FD, James BD, Baum GN, Thomas CE. 1997. *Detailed manufacturing cost estimates for polymer electrolyte membrane fuel cells for light duty vehicles.* Report. pp. 1–50. Arlington, VA: Directed Technologies

101. Little AD. 2000. *Cost analysis of fuel cell systems for transportation: baseline system cost estimate*. SFAA DE-SCO2–98EE50526, Final report, Washington, DC: US DOE
102. Adams J. 1998. *Fuel cells for transportation program*, Contrac. Annu. Prog. Rept. 1:3. Washington, DC: US DOE
103. Davies DP, Adcock PL, Turpin M, Rowen SJ. 2000. *J. Power Sources* 86:237–42
104. Makkus RC, Janssen AHH, de Bruijn FA, Mallant RK. 2000. *J. Power Sources* 86: 274–82
105. Wind J, Spah R, Kaiser W, Bohm G. 2002. *J. Power Sources* 105:154–58
106. Kim JJ, Peelen JS, Hemmes WHA, Makkus RC. 2002. *Corrosion Sci.* 44: 635–55
107. Hodgson DR, May B, Adcock PL, Davies DP. 2001. *J. Power Sources* 96:233–25
108. Del Rio C, Ojeda MC, Acosta JL, Escudero MJ, Hontanon E, Daza L. 2002. *J. Appl. Polymer Sci.* 83:2817–22
109. Theodore MB, Klett TM, Henry JW, Lara-Curzio JJ. 2000. *J. Electrochem. Soc.* 147:4083–86
110. Hards GA, Ralph TR, Thompsett D, Buchanan JS. 2002. *New catalyst and MEA developments for high performance PEMFCs.* Presented at Fuel Cell Sci. Technol. Amsterdam
111. Igarashi H, Fujino T, Zhu YM, Uchida H, Watanabe M. 2001. *Phys. Chem. Chem. Phys.* 3:306–14
112. Yu HM, Hou ZJ, Yi BL, Lin ZY. 2002. *J. Power Sources* 105:52–57
113. Haug AT, White RE, Weidner JW, Huang W. 2002. *J. Electrochem. Soc.* 149:862–67
114. Escudero MJ, Hontanon E, Schwartz S, Boutonnet M, Daza L. 2002. *J. Power Sources* 106:206–14
115. Schmidt TJ, Jusys Z, Gasteiger HA, Behm RJ, Endruschat U, Boennemann H. 2001. *J. Electroanal. Chem.* 501:132–40
116. Starz KA, Auer E, Lehmann Th, Zuber R. 1999. *J. Power Sources* 84:167–72
117. Denis MC, Lalande G, Guay D, Dodelet JP, Schulz R. 1999. *J. Appl. Electrochem.* 29:951–60
118. Gouerec P, Denis MC, Guay D, Dodelet JP, Schulz R. 2000. *J. Electrochem. Soc.* 147:3989–96
119. Toda T, Igarashi H, Watanabe M. 1999. *J. Electroanal. Chem.* 460:258–62
120. Paulus UA, Wokaun A, Scherer GG, Schmidt TJ, Stamenkovic V, et al. 2002. *J. Phys. Chem. B* 106:4181–91
121. Handley C, Brandon NP, van der Vorst R. 2002. *J. Power Sources* 106:344–52
122. Jones DJ, Roziere J. 2001. *J. Membr. Sci.* 185:41–58
123. Hasiotis C, Deimede V, Kontoyannis C. 2001. *Electrochim. Acta* 46:2401–6
124. Staiti P, Minutoli M, Hocevar S. 2000. *J. Power Sources* 90:231–35
125. Xing B, Savadogo O. 2000. *Electrochem. Commun.* 2:345–49
126. Kosmala B, Schauer J. 2002. *J. Appl. Polymer Sci.* 85:1118–27
127. Hasiotis C, Qingfend L, Deimede V, Kallitsis JK, Kontoyannis CG, Bjerrum NJ. 2001. *J. Electrochem. Soc.* 148:A513–19
128. Schechter A, Savinell RF. 2002. *Solid State Ionics* 147:181–87
129. Bae J-M, Honma I, Murata M, Yamamoto T, Rikukawa M, Ogata N. 2002. *Solid State Ionics* 147:189–94
130. Staiti P, Minutoli M. 2001. *J. Power Sources* 94:9–13
131. Lopez ML, Compan V, Garrido J, Riande E, Acosta JL. 2001. *J. Electrochem. Soc.* 148:E372–77
132. Genova-Dimitrova P, Baradie B, Foscallo D, Poinsignon C, Sanchez JY. 2001. *J. Membr. Sci.* 185:59–71
133. Antonucci PL, Ariso AS, Creti P, Rammunni F, Antonucci V. 1998. *Solid State Ionics* 125:431–37
134. Zoppi RA, Yoshida IVP, Nunes SP. 1998. *Polymer* 39:1309–15
135. Deleted in proof
136. Walker CW. 2002. *J. Power Sources* 110: 144–51
137. Adjemian KT, Srinivasan S, Benziger J,

Bocarsly AB. 2002. *J. Power Sources* 109:356–64
138. Costamagna P, Yang C, Bocarsly AB, Srinivasan S. 2002. *Electrochim. Acta* 47: 1023–33
139. Kerres J, Ullrich A, Meier F, Haring T. 1999. *Solid State Ionics* 125:243–49
140. Zhang W, Tone C-M, Kerres J. 2001. *Sep. Pur. Tech.* 22-23:209–21
141. Guo QN, Pintauro P, Tang H, O'Connor S. 1999. *J. Membr. Sci.* 154:175–81
142. Kreuer KD. 2001. *J. Membr. Sci.* 185:29–39
143. Zaidi SMJ, Mikhailenko SD, Robertson GP, Guiver MD, Kaliaguine S. 2000. *J. Membr. Sci.* 173:17–34
144. Miyake N, Wainright JS, Savinell RF. 2001. *J. Electrochem. Soc.* 148:A905–9
145. Doyle M, Choi SK, Proulx G. 2000. *J. Electrochem. Soc.* 147:34–37
146. Nogami M, Usui Y, Kasuga T. 2002. *Fuel Cells* 1:181–85
147. Yang T-H, Yoon Y-G, Kim C-S, Kwak S-H, Yoon K-H. 2002. *J. Power Sources* 106:328–32
148. Nakajima H, Nomura S, Sugimoto T, Nishikawa S, Honma I. 2002. *J. Electrochem. Soc.* 149:A953–59
149. Ahmed S, Krumpelt M. 2001. *Int. J. Hydrogen Energy* 26:291–301
150. Joensen F, Rostrup-Nielsen JR. 2002. *J. Power Sources* 105:195–201
151. Urban PM, Funke A, Muller JT, Himmen M, Docter A. 2001. *Appl. Catalysis A* 221:459–70
152. Jiang C. 1995. *Chem. Eng. Technol.* 18:1
153. Schneider M, Kochloeft K, Pohl J. 1984. *Eur. Patent No. 0126425*
154. Gorte RJ, Graham GW, Bunluesin T. 1998. *Appl. Catalysis B* 15:107–14
155. Nagano S. 2001. *Energy Conversion Manage.* 42(15–17):1817–29
156. Dicks AL. 1996. *J. Power Sources* 61: 113–24
157. Dicks AL. 1998. *J. Power Sources* 71: 111–22
158. Aguiar P, Chadwick D, Kershenbaum L. 2002. *Chem. Eng. Sci.* 57:1665–77
159. Aguiar P, Lapena-Rey N, Chadwick D, Kershenbaum L. 2001. *Chem. Eng. Sci.* 56:651–58
160. Priestnall MA, Kotzeva VP, Fish DJ, Nilsson EM. 2002. *J. Power Sources* 106:21–30
161. Vollmar H-E, Maier C-U, Nolscher C, Merklein T, Poppinger M. 2000. *J. Power Sources* 86:90–97
162. Micheli PL, Williams MC, Sudhoff FA. 1996. *U.S Patent No. 5,541,014*
163. Dyer CK. 2002. *J. Power Sources* 106:31–34